

When there is a discrepancy between the information in this technical report and information in JDox, assume JDox is correct.



**STScI** | SPACE TELESCOPE  
SCIENCE INSTITUTE

## JWST TECHNICAL MEMORANDUM

<p>Title:</p> <p><b>OTE Science Performance Memo 3</b></p> <p><i>Detection and Correction of a Uniquely Large Mirror Shift during Cycle 2.</i></p>	<p>Doc #: JWST-STScI-008650</p> <p>Date: 03/12/2024</p> <p>Rev: -</p>
<p>Authors: Marshall D. Perrin, Matthew Lallo, Randal Telfer, Nicolas Flagey, Marcio Meléndez, Charles-Philippe Lajoie, Thomas M. Comeau, Bernard A. Kulp, Tracy Beck, Gregory R. Brady</p>	<p>Release Date: 13 March 2024</p>

### Table of Contents

1.0	Introduction.....	2
2.0	Detection and Correction of the Large Wing Tilt Event.....	4
2.1	The effect of “Phase Wrapping” on wavefront sensing.....	5
2.2	Effects on Point Spread Functions.....	7
3.0	Generating Model PSFs for Calibrating Science Data .....	10
4.0	Timing and Chronology .....	11
5.0	Conclusion .....	12

## 1.0 INTRODUCTION

Since JWST's successful alignment and commissioning, the telescope's mirrors continue to be monitored roughly every 48 hours, allowing for corrections as needed to maintain image quality. See [Lajoie et al. 2023](#) for a summary of this wavefront sensing and control (WFSC) monitoring and maintenance program during cycle 1.

A particular source of wavefront variation is the so-called "tilt event", i.e. occasional abrupt shifts in mirror positions thought to be caused by stick-slip release of stored stresses from thermal contraction during cooldown. Overall, the frequency of these occasional events has decreased since commissioning, but they still occur, unpredictably, from time to time. See Figure 1. These tilt events are most often seen in the two sets of "wing" segments comprising the left and right sides of the telescope's primary mirror. They are believed to arise from the release of stored stresses in the hinge and latch interfaces for the deployable wings. Typically, the measured wavefront stability is below  $< 10\text{-}20$  nm over the 2-day observation cadence; often well below 10 nm. Wavefront misalignment from such small shifts accumulates over time, and eventually reaches the threshold for a mirror correction. A few times a year, there have been larger tilt events of  $\sim 100$  nm rms; these are corrected expeditiously after detection, in the subsequent WFSC visit 48 hours later. The largest prior shift observed was on 2022 July 12, when there was a 240 nm rms shift affecting the left (-V2) wing, especially segment B5. Consistently throughout flight, this left wing (comprising segments B5, C5, and B6) has been the portion of the telescope most affected by tilt events.

The 2024 Feb 27 WFS measurement detected a shift in positions of these wing segments larger than had been seen previously. Analyses eventually determined that segment C5 had shifted in position by nearly 1 micron. This is the first (and thus far only) time that a shift has resulted in the OTE wavefront temporarily exceeding its requirement specification<sup>1</sup>. After the discovery of this misalignment, it was immediately corrected in two stages over the next few days during the first available correction opportunities.

**After these corrections, the telescope alignment and image quality are once again nominal, with no lasting effect.** However, some science data taken during this time period was inevitably affected, and the JWST mission operations staff communicated rapidly to the affected PIs. This memo is intended in part to provide additional information to those science teams and the broader community.

We note that the WFS analyses clearly indicate no change to any mirror surface figure during this event. This rules out any potential micrometeorite strike on the front surface of any segment as a cause for this event. The mirrors on that wing moved in 3D position only, in a way that would also be consistent with a slip orthogonal to the wing latch interface.

Engineering analyses of the underlying physical root cause for this large wing event continue and may be reported elsewhere. **This document focuses on the immediate specifics of what was measured, how it was corrected, and the effects on science data.**

---

<sup>1</sup> Recall that the telescope wavefront error requirement is 135 nm rms. In comparison, the achieved mirror alignment is typically in the range 60-70 nm rms. The total wavefront at any instrument field point will be somewhat larger than this, the sum of the telescope and instrument wavefront errors.

**JWST Wavefront Monitoring & Maintenance:  
2024-03-03 to 2024-03-08**

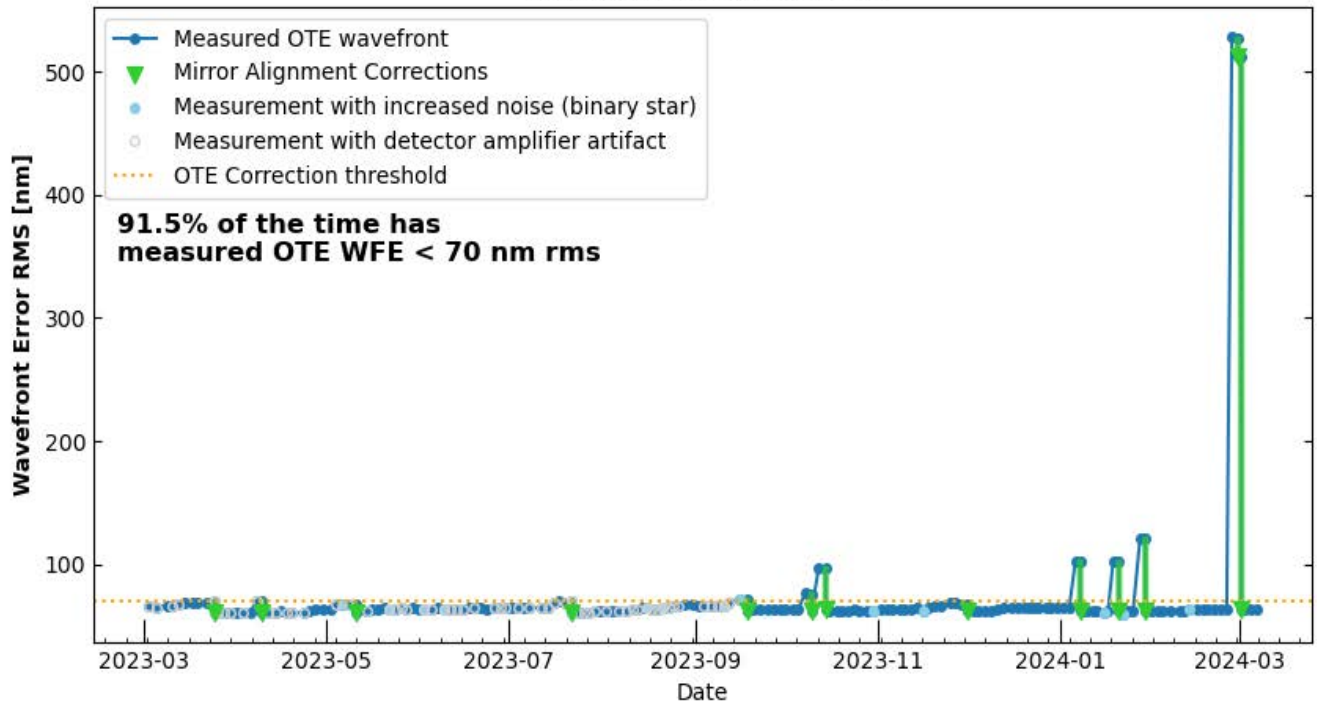


**Figure 1:** Time series of measured telescope root mean square (RMS) wavefront error. The outlier nature of the 2024 Feb event is clear. The observed change in wavefront is many times larger than seen in other events during science operations. The previous largest event was a 240 nm rms mirror move on 2022 July 12, not shown.

## **2.0 DETECTION AND CORRECTION OF THE LARGE WING TILT EVENT**

The large shift of the left ( $-V2$ ) wing segments was discovered in the WFS measurement on 2024 Feb 27. Wavefront sensing observation 4504:148 occurred onboard starting at roughly 06:00 UTC, and some hours later the data was downlinked to the ground and automatically processed by the Wavefront Sensing Subsystem (WSS). The wavefront team was alerted to the anomalously large wavefront error at 16:49 UTC (10:49 am Baltimore local time), and immediately convened to analyze and prepare a correction plan. That initial measurement indicated a wavefront error above 500 nm rms, well above any previously observed tilt event.

The large shift of segments B5, C5, and B6 is immediately apparent even in the raw wavefront sensing defocused weak lens images (see Figure 2, top row, second panel). The measurement shows substantial tilts on B5 and B6 in opposite directions, along with a significant piston and tilt on C5. These motions are large enough to “unstack” those segments away from the other 15, resulting in an obviously significantly aberrated PSF (see Figure 2, bottom row, second panel).

A subsequent reconstruction of the chronology of events (detailed in Section 4) indicates that the actual time of the mirror shift had occurred earlier, in the range Feb 25 19:43:29.8 UTC to Feb 25 20:02:56.4 UTC, apparently occurring during the slew between observations 3964:160 and 3596:2.

Mirror correction commands were delivered to flight operations at 17:50 UTC (1:50 pm Baltimore time), and uplinked to the spacecraft along with a revised observing plan on Feb 28 03:10 UTC (11:10 pm Baltimore local time). The correction was performed in the next WFSC visit 4556:1, on Feb 29 starting around 04:00 UTC. This was the first available correction opportunity given the planned 48 hour cadence for JWST WFSC visits.

Given the magnitude of the wavefront error, the team recognized there was the possibility of a “phase wrap” (see next section), and therefore opted to include additional sensing with NIRCcam filter F187N in that first correction visit. Including wavefront sensing with multiple wavelengths provides an enhanced measurement capability, and is the way to identify and quantify a phase wrap. Also because of this possibility, the operations team replanned the observing schedule to add an extra WFSC visit 24 hours later, again with the added F187N filter, to allow immediate correction of any residuals or phase wrap after the first correction.

This preparation in fact allowed our detection of phase wrapping, and its correction 24 hours later. Segment C5’s piston offset was sufficiently large that it exceeded the range of routine wavefront sensing, resulting in an ambiguous initial measurement of its piston (as described more below, routine wavefront sensing cannot distinguish between e.g., +0.2 waves or -0.8 waves of wavefront error). Analysis of the multi-wavelength sensing in visit 4556:1 indicated that segment C5 was indeed “wrapped”, displaced in piston by one half-wavelength from its desired alignment. Mirror correction commands for this were delivered to operations on Feb 29 17:50 UTC, uplinked, and ran on board in WFSC visit 4556:2 starting around 2029 Mar 1 09:20 UTC. **This successfully returned JWST’s mirrors to nominal alignment, with a post-correction measured wavefront error once again below 70 nm rms.**

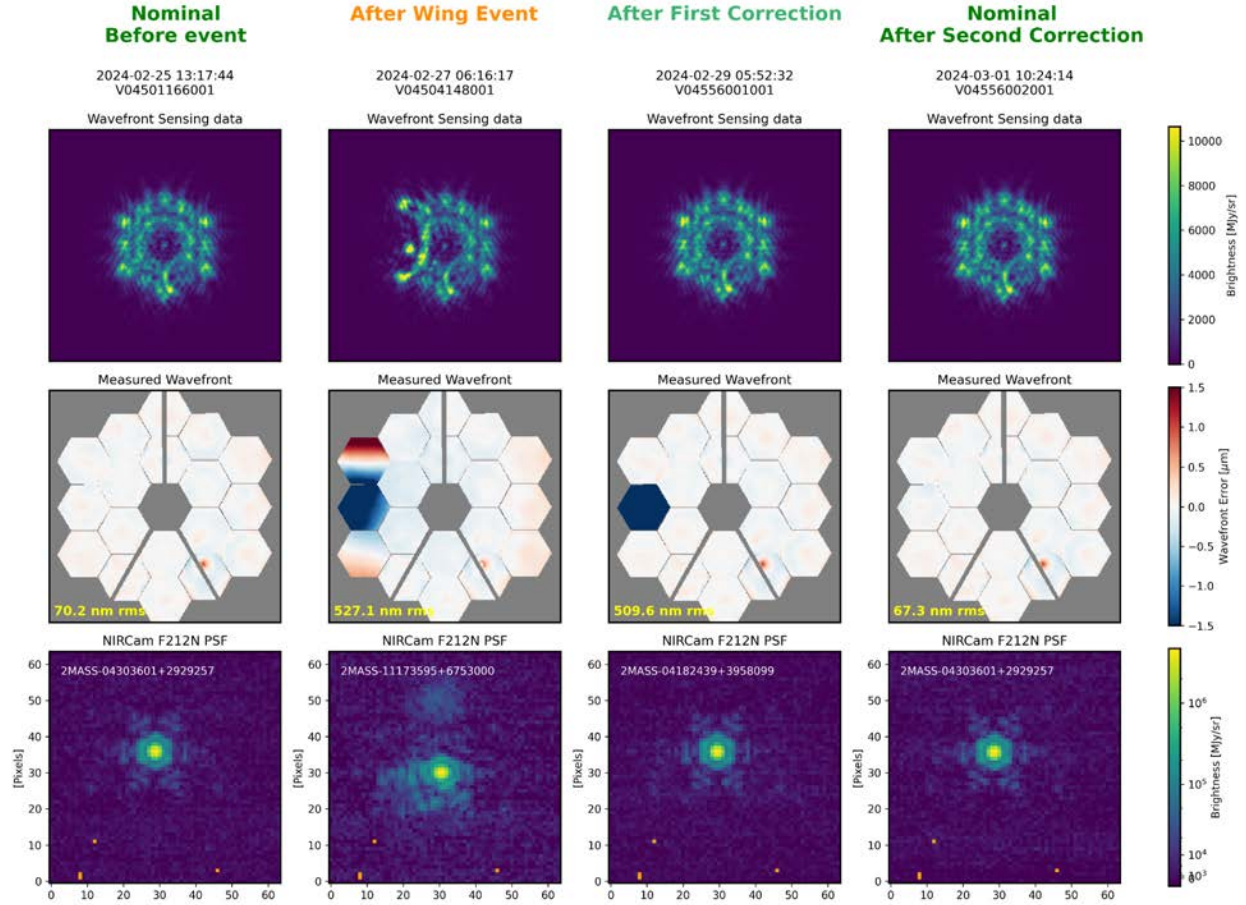


**Figure 2:** Top: wavefront sensing measurements using the WLP8 weak lens in F212N. Middle: derived wavefront maps showing the mirror positions, including the large negative piston on C5 which was not initially inferred due to phase wrapping. Bottom: corresponding NIRCам SW PSFs in F212N for this time period. The WLP8 data have been reoriented to the same orientation as the wavefront maps, which depict JWST “as if standing in front of it looking at the telescope”. The wavefront maps shown for the 2nd through 4th columns are the result of multiwavelength analyses also including the F187N sensing data (not shown).

## 2.1 THE EFFECT OF “PHASE WRAPPING” ON WAVEFRONT SENSING

Since light is a wave phenomenon, a wavefront offset of an integer number of waves yields the same phase of the wavefront. For a reflective system like JWST, a mirror segment physically pistoned by one half a given wavelength will produce an advanced or delayed phase of one full wavelength in the light arriving at the focal surface. Such a full wavelength error, or any integer multiple of it, is referred to as "phase wrapping" and will have no effect on the PSF at that given wavelength. Conversely, a phase error of a half wavelength will have the most pronounced effect at that wavelength, just as the input to a sine function returns the identical output every even number of  $\pi$  but changes sign every odd number of  $\pi$ . (See Figure 3).

The phase wrapping effect is therefore wavelength-dependent with cyclically varying degrees of impact in the image plane, varying in a continuous way between the aforementioned extremes.

The phase wrapping concept has practical implications for JWST WFSC. Our routine WFS is performed at  $\lambda_0=2.12 \mu\text{m}$ . From this we can determine a physical displacement of a mirror segment with great precision, so long as such displacements are significantly smaller than about half the  $2.12 \mu\text{m}$  wavelength. Normally during science operations typical mirror motions at  $\sim < 10 - 20$  nanometers are indeed well within that regime.

In the case of the large tilt observed on 2024 Feb 27, the piston displacement of segment C5 was reported by the analysis to be  $+0.27$  micron, a significant fraction of a half-wave. This indicated for us a possibility of its being “phase wrapped”.

Performing WFS at another wavelength can break  $n*2\pi$  ambiguity and help sense larger pistons correctly (Figure 3). JWST’s WFSC subsystem (WSS), using NIRCcam, has been designed to include the capability to sense at two wavelengths ( $\lambda_0=2.12 \mu\text{m}$ ,  $\lambda_1=1.87 \mu\text{m}$ ). We do not routinely do this since it increases the non-science time spent performing sensing, and is nearly always unnecessary given the usual mirror motion amplitudes.

Realizing from the 2024 Feb 27 sensing that phase wrapping was a possibility, we included the supplemental  $1.87 \mu\text{m}$  sensing in the next two WFSC visits. The first of those applied a  $-0.27 \mu\text{m}$  piston correction to segment C5, but after that correction the post-move confirmation sensing indicated there was indeed a  $2\pi$  phase wrapping remaining. Therefore the second of those two visits performed the “unwrapping” of C5 by applying a  $+1.06 \mu\text{m}$  piston correction.

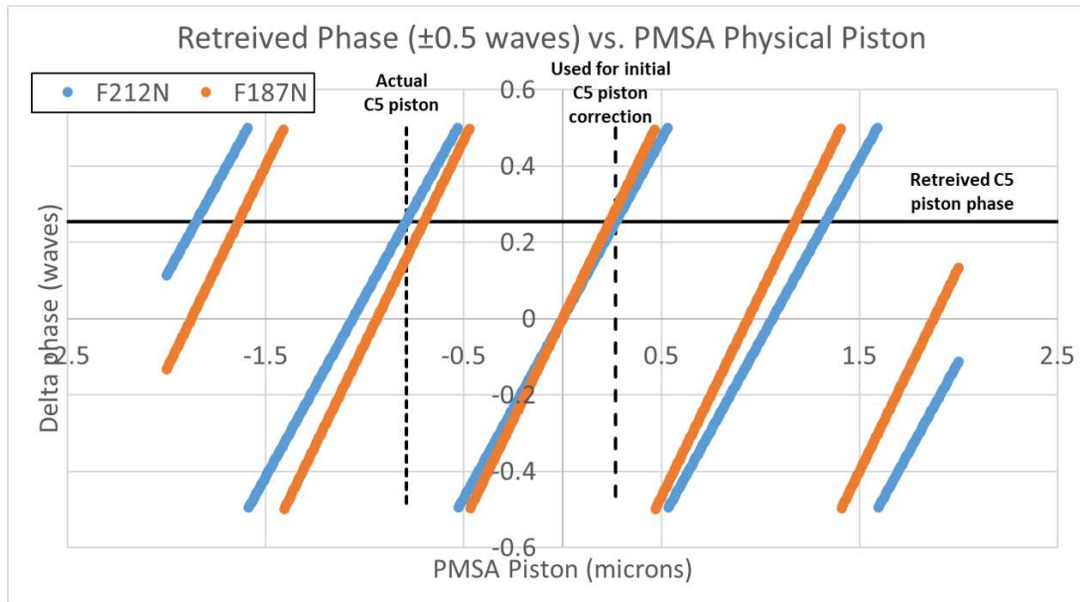


**Figure 3:** Conceptual diagram of phase wrapping. Because the output of the retrieval process is the relative phase of the wavefront, segment piston in the WFE can only be resolved to  $\pm 0.5$  waves, which is assumed not to be exceeded during normal operations. For larger WFE, the phase wraps around: the same apparent phase at  $2.12 \mu\text{m}$  can be caused by multiple values of physical piston separated by  $1.06 \mu\text{m}$ . In other words, the retrieved phase (solid black line) could have been caused by any piston value where the blue line for F212N intersects the solid black line, in particular the two pistons marked by vertical dashed lines. Sensing

with a second wavelength provides additional information to break the degeneracy: the phase at  $1.87 \mu\text{m}$  (shown in orange) would be quite different for the two piston values shown with the dashed lines.

**NOTE:** Because of the phase wrapping, some of the initial wavefront measurement data products (OPD files) delivered to MAST were not accurate in the piston value for segment C5. Once the multi-wavelength analyses were completed, improved data products were delivered to MAST on 2024 March 11, and replaced the prior files. Note that the filenames are identical, with the new versions replacing the initial analyses (i.e. similar behavior as for MAST reprocessing of science data). Users who may have retrieved OPD files from MAST prior to this should make sure to retrieve the updated files now online for accurate wavefront information in this time period.

## 2.2 EFFECTS ON POINT SPREAD FUNCTIONS

During the time period immediately after the wing event, PSFs were significantly aberrated, with several segments visibly misaligned.

During the period after the first correction, with the segments aligned but with the C5 phase-wrap remaining, the effect was more subtle, with some but not all wavelengths having nominal PSFs. For broadband science observations seen through filters with some spectral bandpass, the effect on PSFs will naturally be an average over the effect at many individual wavelengths.

Figures 4 through 7 present measurements and simulations to illustrate these effects.

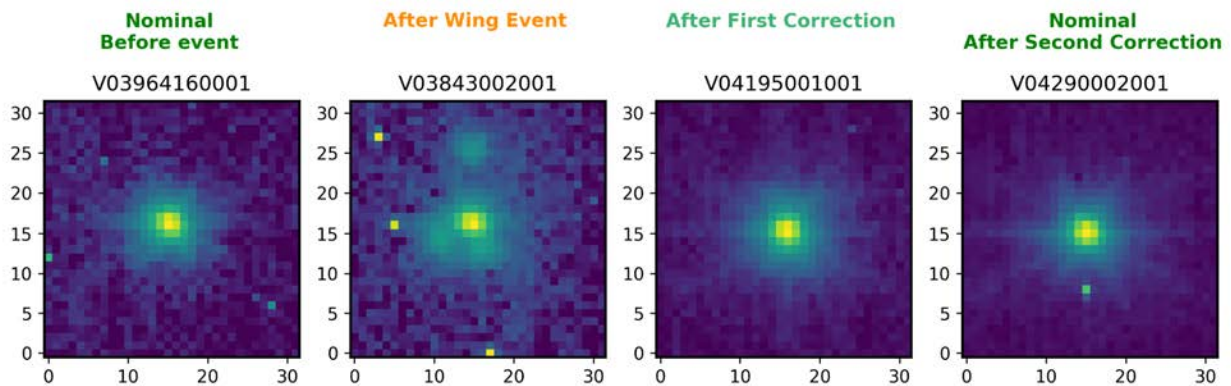


**Figure 4:** Example broadband PSFs as observed with the JWST FGS through this time period. These are FGS “ACQ2” subarray images. The three misaligned segments immediately after the wing event are clearly evident. After the first correction, the observed PSFs were relatively close to nominal again. The FGS spectral bandpass is very broad, from roughly 0.6-5 microns, so the observed appearance sums over many wavelengths. Note the isolated hot pixels (e.g. in rightmost pane) are from the FGS detectors, not the PSF.

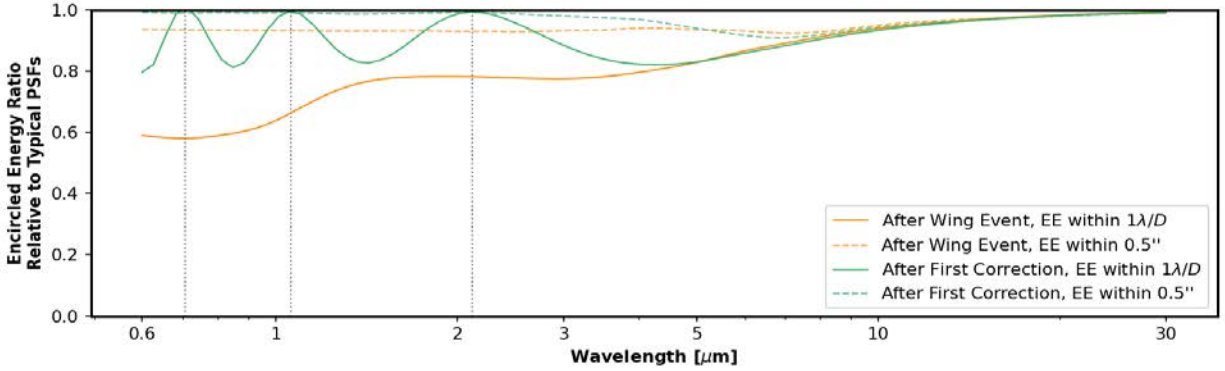


**Figure 5:** Calculations of the reduction in PSF encircled energy as a function of wavelength, compared to nominal JWST PSFs. This is shown for two different radii: within the inner PSF core ( $1 \lambda/D$ ) in solid lines, and within a radius of  $0.5''$  in dashed lines. The loss in encircled energy immediately after the event was substantial. During the period after the first correction when C5 was phase-wrapped, the fraction of light within the PSF core varied strongly as a function of wavelength, but nearly the usual amount of light was within the inner half arcsecond. Users of science data during this time period should be aware that aperture corrections and slit loss models will need custom correction factors for this time period, or else may be off by potentially tens of percent. Note this illustration shows the effect of telescope wavefront error only, leaving out instrument wavefront error and other instrument or detector effects, which could be included in calculations for any specific science dataset.

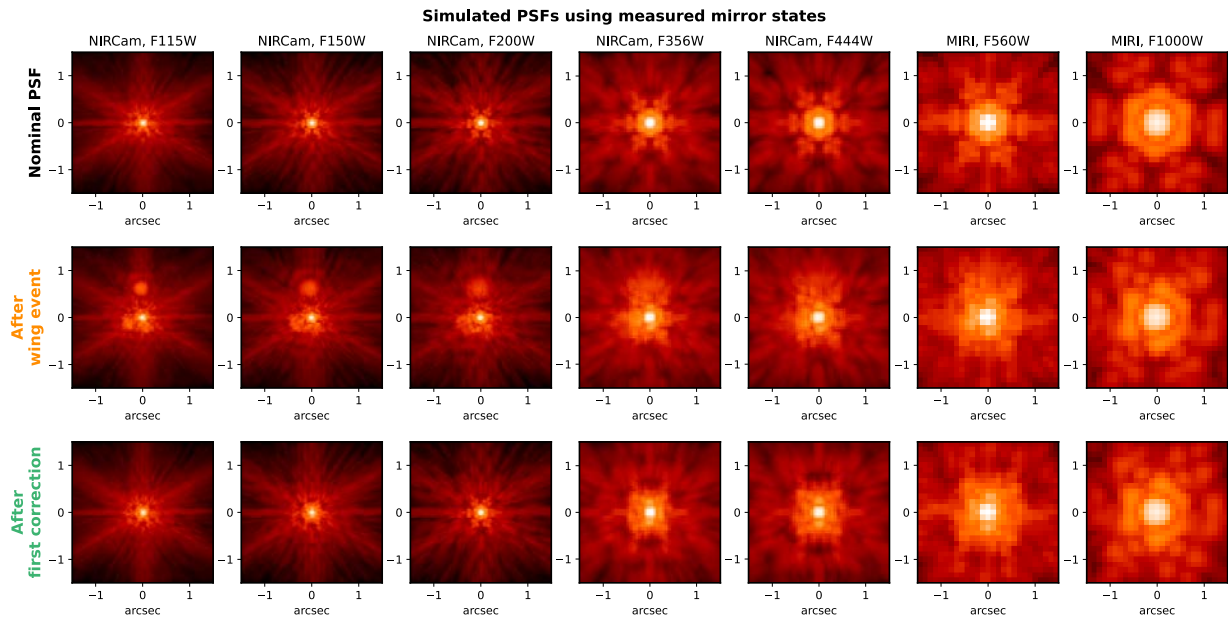


**Figure 6:** Example simulated PSFs in a range of wide-band filters, generated from the WFS measurements as shown above. The top row shows typical JWST PSFs. The second row shows PSFs from the period immediately after the wing event, with obvious misaligned segments at short to medium wavelengths. The large tilt of segment B5 is particularly evident, creating a spot of light about  $0.5''$  in  $+Y$  from the PSF core. The bottom row shows PSFs from the period after the first correction, with segment C5 temporarily phase wrapped. In F200W and F115W, at which the piston offset is close to a multiple of the wavelength, the PSFs are very close to nominal. On the other hand at F150W, or all filters longer than 2 microns, the piston offset was not a multiple of the wavelength, resulting in some aberration to the PSFs. These PSFs are still

relatively sharp, but the inner PSF core is less round and more elongated than the usual JWST PSFs. These displays are on a log stretch with very wide dynamic range to emphasize faint PSF structure and PSF wings.

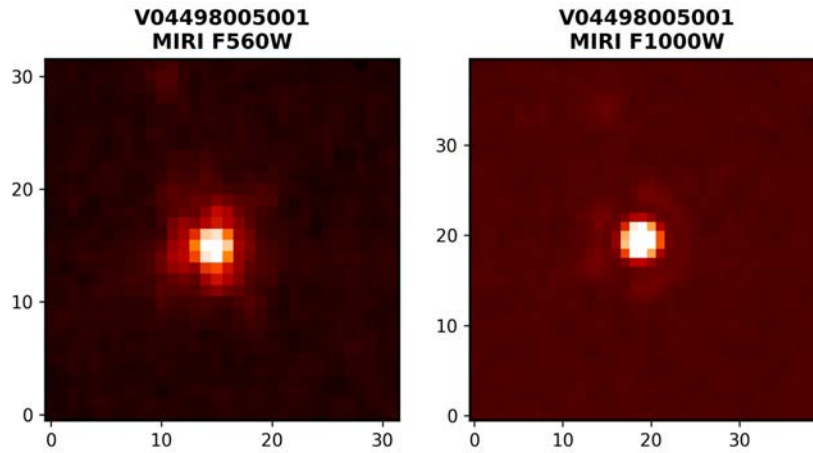


**Figure 7:** Example observed MIRI PSFs from flux calibration observation 4498:5, which happened to be taken shortly after the wing event. These are at the same wavelengths as the two rightmost panels in the second row in Figure 5, above. This is a relatively faint flux standard star at these wavelengths so the SNR in the PSF wings is modest, but some of the same asymmetries can be seen as in the noiseless PSF simulations above. This confirms that long wavelength PSFs during the affected time period were still relatively sharp, though indeed not as symmetric or tight as usual.

### 3.0 GENERATING MODEL PSFS FOR CALIBRATING SCIENCE DATA

Simulated point spread functions can be generated using WebbPSF for the affected time periods. These can be used for instance for deriving improved aperture corrections for photometry, or slit losses for slit spectroscopy, and potentially for deconvolving image data.

General instructions for generating simulated PSFs using in-flight measurements can be found in the WebbPSF documentation at this page:

[https://webbpsf.readthedocs.io/en/latest/jwst\\_measured\\_opds.html](https://webbpsf.readthedocs.io/en/latest/jwst_measured_opds.html)

We briefly repeat here a portion of that Python code for reference.

```
# Create a simulated PSF for a given date

import webbpsf
nrc = webbpsf.NIRCam()
nrc.filter = 'F430M' # or any other desired filter here
nrc.load_wss_opd_by_date('2024-02-26T12:34:56') # date of your observations
psf = nrc.calc_psf(fov_pixels=101)

# The auto-selection by date will find the closest-in-time WFS, which may
# be before or after that science data. This automatic choice is not
# always optimal. If you want to manually select instead, you can do so as
# follows:

nrc.load_wss_opd_by_date('2024-02-26T10:00:00', choice='after')

# create a simulated PSF set up to match some given science file
# The function `setup_sim_to_match_file` automates some of the above steps

miri = webbpsf.setup_sim_to_match_file(
    'jw04290014001_02101_00003_mirimage_cal.fits')
psf = miri.calc_psf(fov_pixels=101)
```

JWST observers may contact the Help Desk for additional assistance in using WebbPSF to model science data during the affected period.

As noted above, some of the initial OPD files delivered during this time period were inaccurate due to phase wrapping, and were subsequently replaced with corrected versions. Users who have prior to 2024 March 13 downloaded OPD files for this time period should delete these from their \$WEBBPSF\_PATH/MAST\_JWST\_WSS\_OPDs directory, and allow WebbPSF to re-download the more accurate versions now on MAST.

#### 4.0 TIMING AND CHRONOLOGY

The period of time during which science programs may have seen the degraded PSF resulting from this mirror event can be broken into the following phases:

- From the first observation following the event, to the first wavefront control that was executed (4556:001): the PSF during this period had multiple peaks due to the tilts of three segments (see Figures 4 and 6 above)
- From the first program after the first wavefront control was executed (4556:001) to the execution of the second wavefront control (4556:002): the PSF during this period was comparatively well formed, but with a single segment (C5) having a piston error such that it produced a phase delay of one full wavelength at 2.12  $\mu\text{m}$ , i.e. phase wrapped (described in section 2.1).

**The list below identifies the programs within these periods. The wing tilt event is believed to have occurred on 25 Feb, between 19:43:30 and 20:02:56 UTC during the slew prior to the first program below.**

```
3596:2:1 NIRISS SOSS V-DR-TAU
3254:1:1 MIRI Coron LKCA15
3254:2:1 MIRI Coron LKCA15-SCI-BACKGROUND
3254:3:1 MIRI Coron LKCA15-SCI-BACKGROUND
3254:4:1 MIRI Coron LKCA15-REFERENCE
4201:3:1 NRS IFU IRAS04302-NIRSPEC
4290:13:1 NIRCam Imaging V-HK-TAU
4290:14:1 MIRI Imaging V-HK-TAU
2780:19:1 NRS FS HD-32297
2780:20:1 NIRCam Coron HD-32297
2780:21:1 NIRCam Coron HD-32297
2780:22:1 NIRCam Coron HD-32297-PSF
3947:7:1 NIRCam Coron AB-AUR
3947:8:1 NIRCam Coron AB-AUR
3947:9:1 NIRCam Coron HD-35600
```

#### **4504:148 WFSC ROUTINE**

*(visit that detected the event and was used to create the first mirror control)*

```
3843:2:1 NRS IFU SGAS1110-IFU-POS1
4106:5:1 NRS MOS msa-cat-v2
4106:6:1 NRS MOS msa-cat-v2
4106:7:1 NRS MOS msa-cat-v2
4496:8:1 MIRI Imaging HR5467
3433:1:1 NRS IFU MS1358-ARC
```

4499:92:1 MIRI MRS HD163466  
4499:93:1 MIRI MRS HD163466-BKG  
4498:5:1 MIRI Imaging SNAP-2  
2965:11:1 MIRI LRS WISE1049AB  
2965:12:1 MIRI LRS WISE1049AB  
2965:13:1 NRS BOTS WISE1049AB

#### **4556:001 WFSC ROUTINE**

*(visit that executed the first mirror control and determined C5 was phase-wrapped)*  
**29 Feb ~04:00 UTC**

4195:1:1 NIRSpec Bright Object Time Series  
4290:1:1 NIRCам Imaging  
4290:18:1 MIRI Imaging  
3690:156:1 MIRI Low Resolution Spectroscopy  
3171:13:1 NIRSpec Bright Object Time Series  
2974:4:1 NIRSpec IFU Spectroscopy

#### **4556:002 WFSC ROUTINE**

*(visit that executed the second mirror control to unwrap C5)*  
**01 Mar ~09:00 UTC**

## **5.0 CONCLUSION**

This document provides a summary of the events around this unusual period for the telescope image quality, briefly describes the effects on PSFs, and provides some guidance in factors to consider when assessing or analyzing science data from this time period.

Though this was a surprisingly large outlier event, it was well within the capability of JWST's wavefront sensing and control system to detect and correct, and the telescope was swiftly returned to its usual image quality.

Observers with specific questions for science data in this time period are encouraged to contact the JWST help desk.